Bioorganic & Medicinal Chemistry 19 (2011) 2458–2463

Contents lists available at ScienceDirect

Bioorganic & Medicinal Chemistry

journal homepage: www.elsevier.com/locate/bmc

Per-N-methylated analogues of an antitumor bicyclic hexapeptide RA-VII

Yukio Hitotsuyanagi, Ji-Ean Lee, Saori Kato, Ik-Hwi Kim, Hideyuki Kohashi, Haruhiko Fukaya, Koichi Takeya *

School of Pharmacy, Tokyo University of Pharmacy and Life Sciences, 1432-1 Horinouchi, Hachioji, Tokyo 192-0392, Japan

ARTICLE INFO

Article history:
Received 15 December 2010
Revised 29 January 2011
Accepted 1 February 2011
Available online 5 March 2011

Keywords:
RA-VII
Bouvardin
N-Methylation
X-ray crystallography
Rubia cordifolia
Cytotoxicity

ABSTRACT

Penta-*N*-methyl and hexa-*N*-methyl analogues of RA-VII, an antitumor bicyclic hexapeptide of plant origin, were prepared. In the former, the nitrogens of D-Ala-1 and Ala-4 and in the latter, those of D-Ala-1, Ala-2, and Ala-4 were methylated under the phase-transfer catalysis conditions. Their solution structures were established by NOESY experiments and the crystal structures by X-ray crystallography. Those two methylated analogues showed much weaker cytotoxicity against P-388 leukemia cells than the parent RA-VII.

1. Introduction

RA-VII (**1**),[1,2] isolated from *Rubia cordifolia* L. and *Rubia akane* Nakai (Rubiaceae), and bouvardin (NSC 259968, **2**)[3] from *Bouvardia ternifolia* (Cav.) Schltdl. (Rubiaceae) (Fig. 1) are bicyclic hexapeptides which are structurally closely related to each other, both having potent antitumor activity. Their antitumor action is considered to be due to inhibition of protein synthesis through interaction with eukaryotic ribosomes.[4,5] Recently, peptide **1** was shown to cause conformational change of F-actin and induce G2 arrest through the inhibition of cytokinesis.[6] These peptides exist as a mixture of two or three stable conformers in solution,[7,8] and the most populated conformer of **1**, having *trans*, *trans*, *trans*, *trans*, *cis*, and *trans* (*t*-*t*-*t*-*t*-*c*-*t*) configuration in the peptide bonds between D-Ala-1/Ala-2, Ala-2/Tyr-3, Tyr-3/Ala-4, Ala-4/Tyr-5, Tyr-5/Tyr-6, and Tyr-6/D-Ala-1, respectively, has been identified as an active conformer.[9–11] In this conformer, the intramolecular hydrogen bondings between D-Ala-1 C=*O* and Ala-4 N*H* and between Ala-4 C=*O* and D-Ala-1 N*H* contribute to the stabilization of this conformation.[8]

In the present work, to study the roles and meanings of those intramolecular hydrogen bondings or of the backbone peptide conformation in the biological activities of **1**, we prepared its N-methylated analogues, **3** and **4**, in which the amide protons of D-Ala-1 and Ala-4 were replaced by methyl groups. In thus prepared **3** and **4**, the intramolecular hydrogen bondings were interfered and their original peptide backbone conformations were affected as expected. Their new backbone conformation and their cytotoxicity were studied.

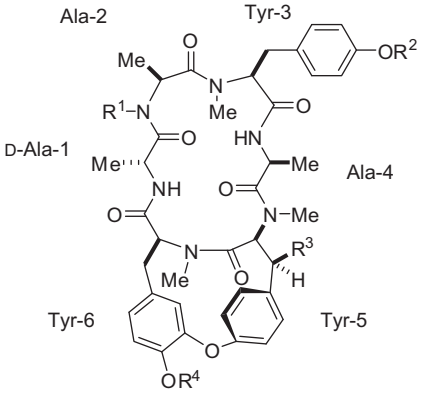

RA-VII (**1**): $R^1 = R^3 = H$, $R^2 = R^4 = Me$
Bouvardin (**2**): $R^1 = R^4 = H$, $R^2 = Me$, $R^3 = OH$
5: $R^1 = R^2 = R^4 = Me$, $R^3 = H$
RA-II (**8**): $R^1 = R^2 = R^3 = H$, $R^4 = Me$

Figure 1. Structures of RA-VII (**1**), bouvardin (**2**), analogue **5**, and RA-II (**8**).

* Corresponding author. Tel.: +81 42 676 3007; fax: +81 42 677 1436.
E-mail address: takeyak@ps.toyaku.ac.jp (K. Takeya).

0968-0896/$ - see front matter © 2011 Elsevier Ltd. All rights reserved.
doi:10.1016/j.bmc.2011.02.003

2. Results and discussion

2.1. Preparation of N-methylated analogues 3 and 4

When subjected to the previously known N-methylation procedure by using iodomethane and potassium fluoride–alumina in 1,2-dimethoxyethane[8] or by using iodomethane and 50% aqueous sodium hydroxide with tetrabutylammonium bromide in dichloromethane,[12] **1** produced exclusively mono-methylated product **5**, in which only the nitrogen of Ala-2 was methylated. The N-methylation of **1** at Ala-2 is known to scarcely affect the backbone peptide conformation and the cytotoxic activity.[8,12] The amide proton of Ala-2 is externally oriented and solvent-exposed to be more easily methylated, whereas those of D-Ala-1 and Ala-4 are oriented inward and are involved in the intramolecular hydrogen bonding so that they are less reactive and need stronger reaction conditions for that. When peptide **1** was stirred vigorously with 2 mol equiv of tetrabutylammonium iodide and excess amounts of iodomethane and powdered sodium hydroxide in dichloromethane at room temperature for 24 h, hexa-*N*-methyl product **3** was obtained in 78% yield (Scheme 1). Since **3** did not give good crystals for crystallography, its bromide **3a** was prepared by treating **3** with pyridinium hydrobromide perbromide and sodium acetate in a mixture of methanol and acetic acid. Its X-ray crystallography showed that the stereochemistry of the chiral centers of **3** was the same as that of the parent peptide **1** (Fig. 2). N-Methylation of peptides normally promotes base-catalyzed epimerization at the adjacent C^{α} position.[13] In fact, a simple treatment of **1** with base in a homogeneous medium produced its diastereomers at Tyr-5 or at Tyr-3 and Tyr-5.[14] The present N-methylation of peptide **1** to its hexa-*N*-methyl analogue, **3**, under the phase-transfer catalysis (PTC) conditions, however, did not affect the original diastereomeric integrity, which is noteworthy.

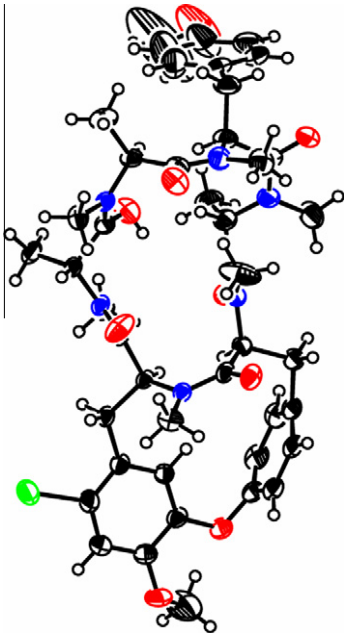

Figure 2. ORTEP representation of analogue **3a**.

Penta-*N*-methyl analogue **4** was prepared by first protecting the most reactive Ala-2 nitrogen before N-methylation. Possible

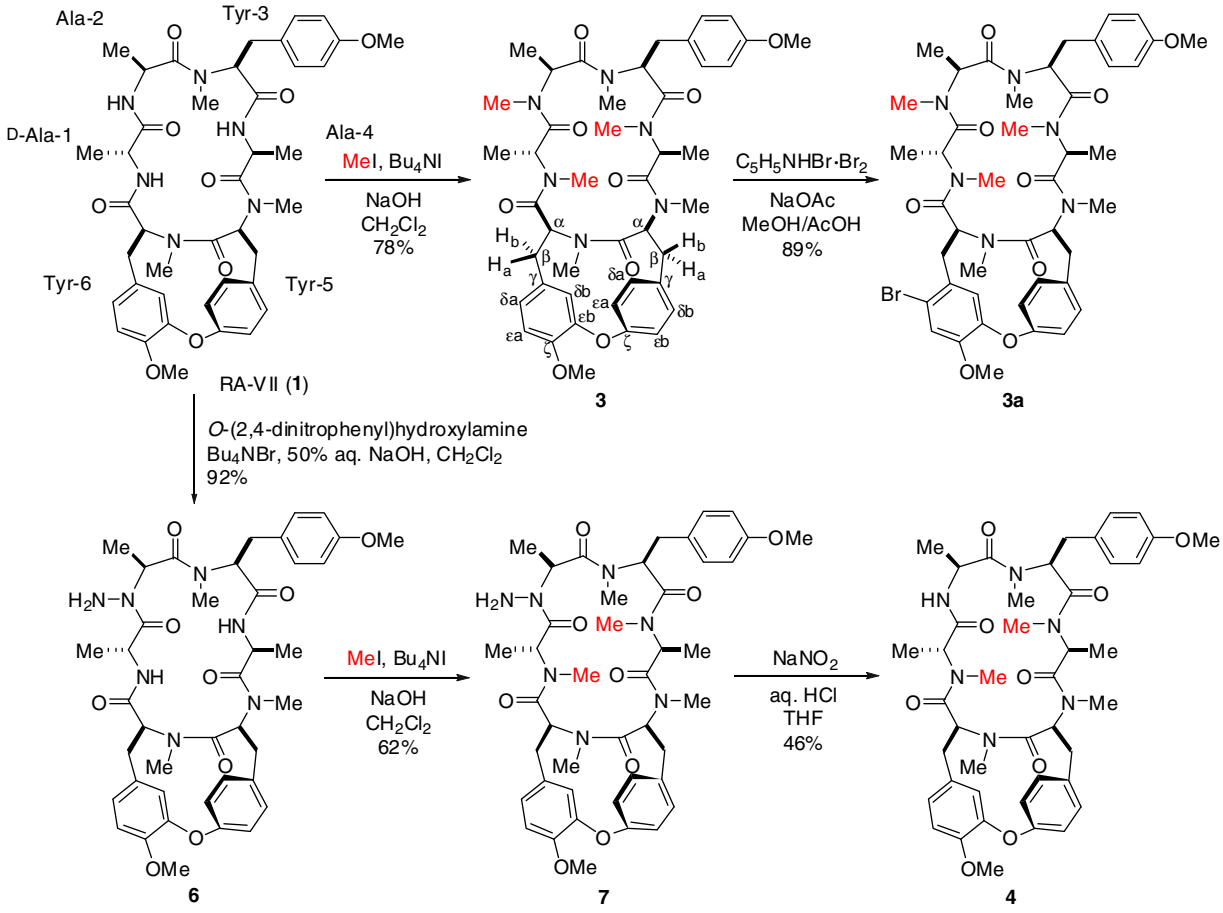

Scheme 1. Preparation of N-methylated analogues of RA-VII.

protecting groups for the peptide nitrogens are very limited, but we found that an *N*-amino group served as a good protecting group in this case. When **1** was treated with *O*-(2,4-dinitrophenyl)hydroxylamine and 50% aqueous sodium hydroxide under PTC conditions, an amino group was effectively introduced on the nitrogen atom of Ala-2 to give an *N*-amino product **6** in 92% yield. The protecting group remained intact during the subsequent N-methylation of **6** with iodomethane and powdered sodium hydroxide under PTC conditions to give **7** in 62% yield. The protecting group at Ala-2 was removed easily when **7** was treated with sodium nitrite in an acidic medium to give penta-*N*-methyl analogue **4** in 46% yield. The X-ray crystallography of **4** confirmed that no changes in the chirality of stereogenic centers in the molecule had occurred through transformations (Fig. 3).

2.2. Structures of 3, 3a and 4 in solution and of 3a and 4 in crystals

The solution structures of **3**, **3a**, and **4**, in which *N*-methyl groups were introduced and accordingly the intramolecular hydrogen bonding and the backbone conformation had been affected, were studied by the NMR experiments. The ^{1}H and ^{13}C NMR spectra of hexa-*N*-methyl analogue **3** in $CDCl_3$ (Tables 1 and 2) demonstrated that it was present in three conformers in a ratio of 93:6:1. In the solution structure of the major conformer of population 93%, the NOE correlations observed between D-Ala-1 H^{α}/Ala-2 NMe and between D-Ala-1 H_3^{β}/Ala-2 NMe showed that the amide bond between D-Ala-1/Ala-2 was *trans*, and the correlation between Ala-2 H^{α}/Tyr-3 H^{α}, that the amide bond between Ala-2/Tyr-3 was *cis* (Fig. 4). Analogously, from the correlations between Tyr-3 H^{α}/Ala-4 H^{α}, Ala-4 H^{α}/Tyr-5 NMe, Tyr-5 H^{α}/Tyr-6 H^{α}, and Tyr-6 H^{α}/D-Ala-1 NMe, the amide bonds between Tyr-3/Ala-4, Ala-4/Tyr-5, Tyr-5/Tyr-6, and Tyr-6/D-Ala-1 were determined to be *cis*, *trans*, *cis*, and *trans*, respectively. Thus, the sequence of the amide configuration of the major conformer of **3** was shown to be *t*-*c*-*c*-*t*-*c*-*t*.

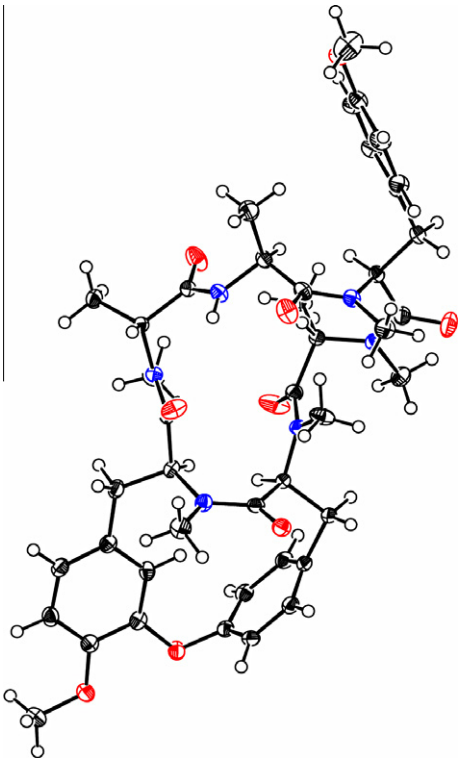

Figure 3. ORTEP representation of analogue **4**.

The NMR spectra including the NOESY spectrum of **3a**, prepared for the X-ray crystallography, were quite similar to those of **3**, indicating that the solution structures of **3** and **3a** were almost identical. Thus, the major conformer of **3a** of population 93% was shown to have the same amide configuration sequence as that of **3**.

The ^{1}H and ^{13}C NMR spectra of penta-*N*-methyl analogue **4** in $CDCl_3$ (Tables 1 and 2) showed that it was present in two conformers in a ratio of 99:1. In the major conformer of population 99%, the NOE correlations between D-Ala-1 H^{α}/Ala-2 NH, Tyr-3 H^{α}/Ala-4 H^{α}, Ala-4 H^{α}/Tyr-5 NMe, Tyr-5 H^{α}/Tyr-6 H^{α}, and Tyr-6 H^{α}/D-Ala-1 NMe indicated that its amide configurations between D-Ala-1/Ala-2, Tyr-3/Ala-4, Ala-4/Tyr-5, Tyr-5/Tyr-6, and Tyr-6/D-Ala-1 were *trans*, *cis*, *trans*, *cis*, and *trans*, respectively. The chemical shift values of the α-protons of Ala-2 and Tyr-3 were so close that the configuration of the amide bond between Ala-2/Tyr-3 could not be determined by the NOESY data. However, it was considered to be *cis*, because the ^{13}C NMR chemical shift of Tyr-3 C^{α} was δ_C 59.3, a value characteristic of a *cis* amide configuration at this position.[8] Accordingly, the sequence of the amide configuration of the major conformer of **4** was considered to be *t*-*c*-*c*-*t*-*c*-*t* as in the major conformer of **3**. The amide configuration between Tyr-3/Ala-4 was *cis* both in **3** and **4**, which is unique, because in the natural RA-series peptides, including **1** from which **3** and **4** were derived, this amide bond normally takes *trans* configuration. Both in the major conformers of **3** and **4**, characteristic NOE correlations were observed between D-Ala-1 H_3^{β}/D-Ala-1 NMe, Tyr-3 NMe/Tyr-5 NMe, Ala-4 NMe/Tyr-5 NMe, and Ala-4 NMe/Tyr-5 $H^{\beta a}$, implying that their peptide backbone structures in $CDCl_3$ were almost identical.

The solid state structures of **3a** and **4** were studied by crystallography and the results were compared with that of RA-II (**8**), which is considered to have conformational property identical to that of **1**, and which displayed weaker antitumor and cytotoxic activities than **1** due to its absence of *O*-methyl group in Tyr-3 (Fig. 1).[15–17] The results showed that the solid state structure of **3a** was basically identical to that in solution of the major conformers of **3** and **3a** as determined by its NOESY experiments in $CDCl_3$, with the amide configuration of *t*-*c*-*c*-*t*-*c*-*t* (Table 3). The distances between the protons (or the nearest methyl protons) in solid state as estimated by X-ray crystallography and the relevant ones involved in the NOE correlations in **3** in $CDCl_3$ solution, which characterize the backbone structure of its major conformer, were as follows: 2.24 Å (D-Ala-1 H_3^{β}/D-Ala-1 NMe), 3.04 Å (D-Ala-1 NMe/Ala-4 H_3^{β}), 2.88 Å (Ala-2 H^{α}/Ala-4 H^{α}), 2.78 Å (Tyr-3 NMe/Tyr-5 NMe), 2.93 Å (Ala-4 NMe/Tyr-5 NMe), and 2.62 Å (Ala-4 NMe/Tyr-5 $H^{\beta a}$). The distances by crystallography were quite reasonable for producing NOE cross-peaks.

The solid state structure of **4** was shown to have the same *t*-*c*-*c*-*t*-*c*-*t* configuration as **3a**, with very similar back bone torsions (Table 3). However, the side-chain torsion angles of Tyr-3, that is, the N–C^{α}–C^{β}–C^{γ} dihedral (χ1), were −163.5(3)° for **3a** and −65.59(19)° for **4**. The presence of the difference in the dihedral angles as demonstrated by superimposing the crystal structures of **3a** and **4** (Fig. 5) was suggested by a series of the NMR data of the major conformers of **3** and **4**. The methyl signal of Ala-2 in **4** resonated at δ_H 0.58, that in **3** at δ_H 1.17, and those in other analogues **3a**, **6**, and **7** at δ_H 1.15–1.43. This rather unusual upfield shift of the Ala-2 methyl signal may be explained by the presence of the Tyr-3 phenyl ring right above the Ala-2 methyl group, as demonstrated in the solid state structure of **4** (Fig. 3). Differences between the chemical shifts and the vicinal coupling constants of the β-protons of Tyr-3 in **3** and **4** also suggested the conformational preferences of their Tyr-3 side chain. The *pro*-*R* β-proton of Tyr-3 in **3** resonated at δ_H 2.70 with $J_{vicinal}$ = 4.9 Hz, whereas that in **4** at δ_H 3.05 with $J_{vicinal}$ = 8.7 Hz, and the *pro*-*S* β-proton of Tyr-3 in **3** resonated at δ_H 3.50 with $J_{vicinal}$ = 9.3 Hz, whereas that in **4** at δ_H 3.11 with $J_{vicinal}$ = 5.4 Hz. There might be subtle differences

Table 1
^{1}H NMR data for the major conformers of **3**, **3a**, **4**, **6**, and **7** in $CDCl_3$ at 300 K[a]

Position		**3** δ_H[b]	**3a** δ_H[c]	**4** δ_H[d]	**6** δ_H[e]	**7** δ_H[f]
D-Ala-1	α	5.10 (q, 7.3)	5.13 (q, 7.4)	4.64 (q, 7.2)	5.25 (qd, 7.2, 6.8)	5.82 (q, 7.4)
	β	1.30 (d, 7.3, 3H)	1.33 (d, 7.4, 3H)	1.26 (d, 7.2, 3H)	1.27 (d, 6.8, 3H)	1.30 (d, 7.4, 3H)
	NMe (NH)	2.92 (s, 3H)	2.93 (s, 3H)	2.81 (s, 3H)	6.41 (d, 7.2)	2.89 (s, 3H)
Ala-2	α	5.73 (q, 7.1)	5.74 (q, 7.1)	4.90[g]	5.24 (q, 7.1)	5.63 (q, 7.0)
	β	1.17 (d, 7.1, 3H)	1.15 (d, 7.1, 3H)	0.58 (d, 6.4, 3H)	1.43 (d, 7.1, 3H)	1.25 (d, 7.0, 3H)
	NMe (NH, NNH_2)	3.34 (s, 3H)	3.36 (s, 3H)	6.80 (d, 8.8)	4.34 (s, 2H)	4.52 (s, 2H)
Tyr-3	α	5.17 (dd, 9.3, 4.9)	5.16 (dd, 9.1, 5.0)	4.89[g]	3.56 (dd, 10.4, 5.3)	5.00 (dd, 9.4, 4.7)
	βa	3.50 (dd, 13.4, 9.3)	3.49 (dd, 13.4, 9.1)	3.11 (dd, 14.3, 5.4)	3.35 (dd, 14.1, 5.3)	3.54 (dd, 13.2, 9.4)
	βb	2.70 (dd, 13.4, 4.9)	2.72 (dd, 13.4, 5.0)	3.05 (dd, 14.3, 8.7)	3.33 (dd, 14.1, 10.4)	2.69[g]
	δ	7.12 (d-like, 8.6, 2H)	7.13 (d-like, 8.7, 2H)	7.08 (d-like, 8.7, 2H)	7.04 (d-like, 8.6, 2H)	7.11 (d-like, 8.6, 2H)
	ε	6.83 (d-like, 8.6, 2H)	6.84 (d-like, 8.7, 2H)	6.84 (d-like, 8.7, 2H)	6.84 (d-like, 8.6, 2H)	6.83 (d-like, 8.6, 2H)
	NMe	2.88 (s, 3H)	2.89 (s, 3H)	2.91 (s, 3H)	2.86 (s, 3H)	2.88 (s, 3H)
	OMe	3.78 (s, 3H)	3.78 (s, 3H)	3.76 (s, 3H)	3.80 (s, 3H)	3.78 (s, 3H)
Ala-4	α	5.20 (q, 6.4)	5.21 (q, 6.4)	4.19 (q, 6.5)	4.73 (dq, 7.6, 6.7)	5.21 (q, 6.5)
	β	1.15 (d, 6.4, 3H)	1.16 (d, 6.4, 3H)	1.36 (d, 6.5, 3H)	1.07 (d, 6.7, 3H)	1.16 (d, 6.5, 3H)
	NMe (NH)	2.75 (s, 3H)	2.76 (s, 3H)	2.80 (s, 3H)	6.69 (d, 7.6)	2.75 (s, 3H)
Tyr-5	α	4.82 (dd, 10.3, 2.3)	4.81 (dd, 10.3, 2.2)	4.99 (dd, 10.5, 2.2)	5.44 (dd, 11.3, 2.9)	4.78 (dd, 10.3, 2.4)
	βa	2.81 (dd, 10.7, 2.3)	2.85 (dd, 10.7, 2.2)	2.69[g]	2.62 (dd, 11.3, 2.9)	2.91[g]
	βb	3.45 (t, 10.5)	3.43 (t, 10.6)	3.51 (t, 10.6)	3.69 (t, 11.3)	3.39 (t, 10.3)
	δa	7.26 (dd, 8.5, 2.2)	7.27 (dd, 8.4, 2.1)	7.28 (dd, 8.4, 2.2)	7.27 (dd, 8.4, 2.2)	7.25 (dd, 8.4, 2.2)
	δb	7.59 (dd, 8.5, 2.2)	7.62 (dd, 8.4, 2.1)	7.53 (dd, 8.4, 2.2)	7.42 (dd, 8.3, 2.2)	7.61 (dd, 8.5, 2.2)
	εa	6.87 (dd, 8.5, 2.4)	6.88 (dd, 8.4, 2.5)	6.88 (dd, 8.4, 2.5)	6.88 (dd, 8.4, 2.4)	6.88 (dd, 8.4, 2.5)
	εb	7.19 (dd, 8.5, 2.4)	7.16 (dd, 8.4, 2.5)	7.20 (dd, 8.4, 2.5)	7.21 (dd, 8.3, 2.4)	7.18 (dd, 8.5, 2.5)
	NMe	2.50 (s, 3H)	2.52 (s, 3H)	2.57 (s, 3H)	3.10 (s, 3H)	2.51 (s, 3H)
Tyr-6	α	4.66 (dd, 11.9, 3.8)	4.62 (dd, 12.2, 3.1)	4.67 (dd, 12.1, 3.5)	4.56 (dd, 12.1, 3.8)	4.65 (dd, 11.9, 3.6)
	βa	2.97 (dd, 18.2, 11.9)	2.98 (dd, 18.7, 12.2)	2.96 (dd, 18.2, 12.1)	3.13 (dd, 18.0, 12.1)	2.99 (dd, 18.4, 11.9)
	βb	2.86 (dd, 18.2, 3.8)	2.66 (dd, 18.7, 3.1)	2.79[g]	2.95 (dd, 18.0, 3.8)	2.89[g]
	δa	6.59 (dd, 8.4, 2.1)		6.59 (dd, 8.3, 1.9)	6.58 (dd, 8.3, 2.0)	6.60 (dd, 8.3, 2.1)
	δb	4.48 (d, 2.1)	4.51 (s)	4.45 (d, 1.9)	4.35 (d, 2.0)	4.48 (d, 2.1)
	εa	6.81 (d, 8.4)	7.05 (s)	6.81 (d, 8.3)	6.80 (d, 8.3)	6.81 (d, 8.3)
	NMe	2.68 (s, 3H)	2.66 (s, 3H)	2.68 (s, 3H)	2.72 (s, 3H)	2.68 (s, 3H)
	OMe	3.93 (s, 3H)	3.94 (s, 3H)	3.93 (s, 3H)	3.94 (s, 3H)	3.93 (s, 3H)

[a] Recorded at 500 MHz, chemical shifts referenced to residual $CHCl_3$ (7.26 ppm); *J*-values given in Hz in parentheses.
[b] Mixture of one major and two minor conformers in a ratio of 93:6:1.
[c] Mixture of two conformers in a ratio of 93:7.
[d] Mixture of two conformers in a ratio of 99:1.
[e] Mixture of two conformers in a ratio of 97:3.
[f] Mixture of two conformers in a ratio of 92:8.
[g] Multiplicity patterns were unclear due to signal overlapping.

between the peptide backbone structures of **3** and **4**, which might be responsible for such difference in their side chain torsion.

The unique structural features of **3** and **4** were highlighted by superimposing the crystal structures of **3a** and **4** over that of RA-II (**8**), having essentially the same solid state structure as that of their parent antitumor peptide **1** (Fig. 5). The part of the peptide backbone at residues 1–4 in **3a** and **4** significantly deviated form that of **8**, as expected by the difference in the configurations between Ala-2/Tyr-3 and between Tyr-3/Ala-4, which were *cis* and *cis* in **3a** and **4**, and *trans* and *trans* in **8**.

2.3. Cytotoxicity

Analogues **3**, **3a**, **4**, **6**, and **7** prepared in the present study, and, as reference, **1**, were evaluated for their cytotoxicity against P-388 leukemia cells, and the results are summarized in Table 4. Of them, only the *N*-amino analogue **6** retained the potent cytotoxicity of the original peptide **1**, whereas the others **3**, **3a**, **4**, and **7**, having *N*-methyl groups at D-Ala-1 and Ala-4, showed significantly reduced activity.

3. Conclusion

In antitumor bicyclic hexapeptides of RA series, the hydrogen bondings between D-Ala-1 and Ala-4 take an active part in retaining the conformation considered to be the active form of the molecule. In the present study, to further relate the meanings of the hydrogen bondings or of the conformation and its relation to the activity, we prepared a series of analogues of **1** in which the amide nitrogens of D-Ala-1 and Ala-4 were methylated. Introduction of methyl groups and interfering of the hydrogen bonding led to generation of unique backbone structures not observed in the natural RA-series peptides. In those analogues, the *N*-methyl group at Ala-2 affected the side-chain torsion angles of Tyr-3. The quite obvious differences in the 18-membered peptide backbone between **3a** and **4**, and **8** as demonstrated in Figure 5 may give further information about the peptide conformation–activity relationships and also about the effect of different groups on the three-dimensional molecular structures.

4. Experimental

4.1. General

Melting points were determined on a Yanaco MP-3 apparatus and recorded uncorrected. Optical rotations were measured on a JASCO P-1030 digital polarimeter. IR spectra were recorded on a JASCO FT/IR 620 spectrophotometer, NMR spectra on a Bruker DRX 500 spectrometer (500 MHz for ^{1}H NMR, 125 MHz for ^{13}C NMR), and mass spectra on a Micromass LCT spectrometer. Single-crystal X-ray analyses were carried out on a Bruker AXS APEX II ULTRA CCD area detector diffractometer with a rotating anode source (Mo Kα radiation, λ = 0.71073 Å). Preparative HPLC was carried out on a Shimadzu LC-6AD pump unit equipped with an

Table 2
^{13}C NMR data for the major conformers of **3**, **3a**, **4**, **6**, and **7** in $CDCl_3$ at 300 K[a]

Position		**3** δ_C	**3a** δ_C	**4** δ_C	**6** δ_C	**7** δ_C
D-Ala-1	α	49.5	49.6	52.2	46.3	49.8
	β	14.6	14.7	14.3	19.6	14.7
	C=O	174.3	174.3	169.8	176.0	176.5
	NMe	31.0	31.0	30.1		31.3
Ala-2	α	45.2	45.2	43.2	48.4	46.3
	β	16.6	16.7	19.7	13.4	15.2
	C=O	172.9	172.9	172.6	172.6	173.8
	NMe	30.7	30.8			
Tyr-3	α	58.4	58.4	59.3[c]	68.1	58.7
	β	37.5	37.5	35.8	32.5	37.4
	γ	128.4	128.5	128.4	130.6	128.4
	δ	130.7[b]	130.7[b]	130.5[b]	130.2[b]	130.6[b]
	ε	114.3[b]	114.4[b]	114.7[b]	114.1[b]	114.4[b]
	ζ	158.8	158.8	159.0	158.5	158.8
	C=O	167.5	167.6	167.4	167.8	167.0
	NMe	29.7	29.6	29.2	39.6	29.6
	OMe	55.3	55.3	55.4	55.3	55.3
Ala-4	α	54.6	54.6	54.1	46.2	54.7
	β	17.0	17.0	17.5	18.3	16.8
	C=O	169.5	169.6	168.2	171.6	169.4
	NMe	29.1	29.1	29.1		29.1
Tyr-5	α	60.7	60.7	59.2[c]	54.5	60.9
	β	36.6	36.8	36.5	37.0	36.6
	γ	137.1	137.4	136.6	135.4	137.0
	δa	132.6	132.6	132.8	132.8	132.6
	δb	131.4	131.7	131.3	131.0	131.3
	εa	123.5	123.2	123.6	124.2	123.6
	εb	125.9	125.5	126.0	125.9	125.8
	ζ	157.2	156.4	157.3	158.1	157.2
	C=O	169.2	169.4	168.6	169.1	169.4
	NMe	30.1	30.2	29.7	30.5	30.3
Tyr-6	α	54.9	54.9	54.6	57.3	55.2
	β	32.2	33.5	32.0	35.5	32.2
	γ	128.0	127.0	127.8	128.3	128.2
	δa	120.9	114.6	121.0	121.0	120.9
	δb	113.2	113.8	113.0	113.4	113.2
	εa	112.2	116.1	112.3	112.2	112.2
	εb	153.1	152.5	153.0	153.1	153.1
	ζ	146.6	147.3	146.7	146.5	146.5
	C=O	172.5	172.2	172.3	170.3	172.2
	NMe	29.5	29.4	29.4	29.4	29.5
	OMe	56.2	56.4	56.2	56.1	56.2

[a] Recorded at 125 MHz, chemical shifts referenced to $CDCl_3$ (77.03 ppm).
[b] Two carbons.
[c] Assignments may be reversed.

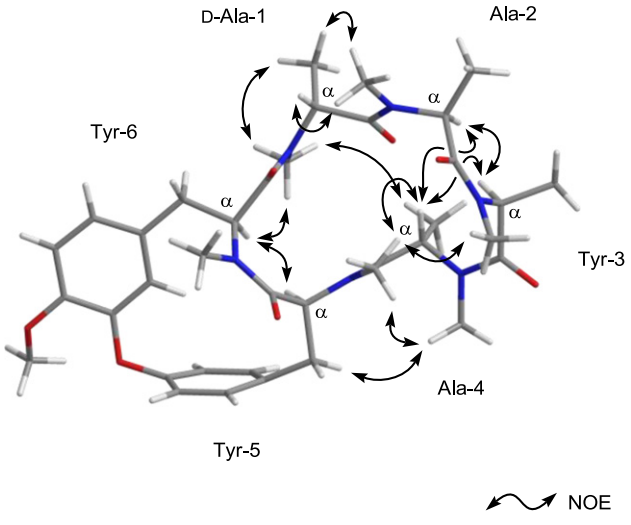

Figure 4. Selected NOE correlations for **3**. The side chain of Tyr-3 was omitted for clarity.

Table 3
X-ray calculated backbone dihedrals (degree) in analogues **3a** and **4**

Residue		**3a**	**4**
D-Ala-1	φ	93.0(3)	97.59(16)
	ψ	−131.8(3)	−89.51(17)
	ω	−173.3(3)	−175.09(14)
Ala-2	φ	−104.4(3)	−151.92(15)
	ψ	121.3(3)	125.20(16)
	ω	2.6(5)	6.6(2)
Tyr-3	φ	−149.1(3)	−129.04(16)
	ψ	89.9(4)	83.44(18)
	ω	11.3(6)	−6.1(2)
Ala-4	φ	−146.6(4)	−137.16(16)
	ψ	67.9(4)	65.10(18)
	ω	−177.4(3)	−171.41(13)
Tyr-5	φ	−152.5(3)	−143.27(14)
	ψ	98.8(3)	92.51(17)
	ω	−20.4(4)	−13.5(2)
Tyr-6	φ	−80.2(4)	−86.03(18)
	ψ	152.0(3)	159.52(14)
	ω	172.5(3)	168.71(13)

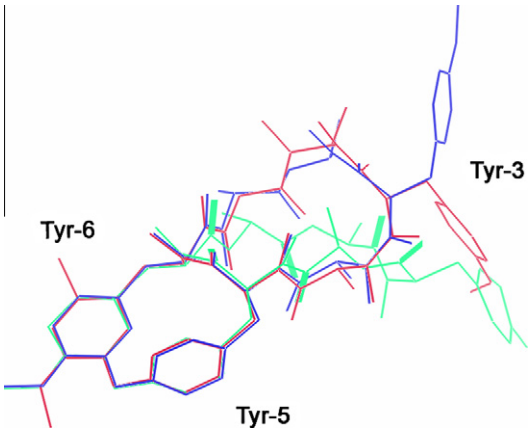

Figure 5. Superposition of the crystal structures of **3a** (red), **4** (blue), and **8** (green).

Table 4
Cytotoxicity of RA-VII (**1**) and analogues **3**, **3a**, **4**, **6**, and **7** against P-388 leukemia cells

Compound	IC_{50} (μM)
RA-VII (**1**)	0.0022
3	3.1
3a	>110
4	10
6	0.0057
7	49

SPD-10A UV detector (254 nm) and an Inertsil ODS-3 column (5 μm, 20 × 250 mm, GL Sciences Inc.), and analytical HPLC with a Sunniest C18 column (5 μm, 4.6 × 250 mm, ChromaNik Technologies Inc.). In vitro cytotoxicity assays were performed as described previously using the P-388 murine lymphocytic leukemia cell line.[10]

4.2. Per-N-methylation of 1

Iodomethane (0.5 mL, 8.0 mmol), tetrabutylammonium iodide (96.0 mg, 0.260 mmol), and powdered NaOH (200 mg, 5.00 mmol) were added to a solution of **1** (100.2 mg, 0.130 mmol) in dichloromethane (1.5 mL), and the mixture was stirred vigorously at room temperature for 24 h. Water (5 mL) was added to the mixture, and the whole was extracted with CH_2Cl_2 (3 × 10 mL). The combined

CH_2Cl_2 extracts were washed sequentially with aqueous hydrochloric acid (2 M, 10 mL) and water (5 mL), dried over sodium sulfate, and filtered, and the solvent removed in vacuo. The residue was subjected to HPLC (MeOH/H_2O 70:30) to give **3** (82.5 mg, 78%) as an amorphous solid, $[\alpha]_D^{26}$ −89 (*c* 0.14, $CHCl_3$). IR (film) ν_{max} 2934, 1650, 1514 cm^{-1}; ^1H and ^{13}C NMR data, in Tables 1 and 2, respectively; HRESIMS *m*/*z* 813.4141 ($[M+H]^+$, calcd for $C_{44}H_{57}N_6O_9$, 813.4187); Analytical HPLC (MeCN/H_2O 55:45, flow rate 0.53 mL/min) 19.1 and 29.8 min.

4.3. Bromination of 3

Sodium acetate (2.7 mg, 0.033 mmol) and pyridinium hydrobromide perbromide (ca. 85%, 12.4 mg, 0.033 mmol) were added to an ice-cooled solution of **3** (18.0 mg, 0.0221 mmol) in a mixture of MeOH/AcOH (1:1, 1 mL). The mixture was stirred at 0 °C for 1 h and then at room temperature for 2 days. The mixture was diluted with $CHCl_3$ (20 mL), washed sequentially with aqueous $NaHSO_3$ (5%, 5 mL) and brine (10 mL), and dried over Na_2SO_4. The mixture was filtered and the solvent removed in vacuo. The residue was subjected to silica gel column chromatography ($CHCl_3$/MeOH 20:1) to afford **3a** (17.5 mg, 89%) as colorless prisms, mp 222–225 °C (MeOH/H_2O), $[\alpha]_D^{26}$ −75 (*c* 0.12, $CHCl_3$). IR (film) ν_{max} 3006, 2935, 1652, 1501, cm^{-1}; ^1H and ^{13}C NMR data, in Tables 1 and 2, respectively; HRESIMS *m*/*z* 891.3354 ($[M+H]^+$, calcd for $C_{44}H_{56}N_6O_9Br$, 891.3292).

4.4. N-Amination of 1

A solution of *O*-(2,4-dinitrophenyl)hydroxylamine (65.1 mg, 0.327 mmol) in dichloromethane (3.5 mL) was added over 1.5 h to a vigorously stirred mixture of **1** (100.8 mg, 0.131 mmol), tetrabutylammonium bromide (21.1 mg, 0.0655 mmol), dichloromethane (3.5 mL), and aqueous NaOH (50%, 1.5 mL). The mixture was further stirred for 1 h. Aqueous KOH (1 M, 20 mL) was added to the mixture, and the whole was extracted with dichloromethane (50 mL). The extract was washed with brine (5 mL), dried over Na_2SO_4, and filtered, and the solvent removed in vacuo. The residue was subjected to silica gel column chromatography (CH_2Cl_2/MeOH 10:1) and then to HPLC (MeOH/H_2O 65:35) to give **6** (94.4 mg, 92%) as colorless needles, mp >300 °C (MeOH/$CHCl_3$), $[\alpha]_D^{25}$ −194 (*c* 0.16, $CHCl_3$). IR (film) ν_{max} 3388, 2934, 1680, 1632, 1513 cm^{-1}; ^1H and ^{13}C NMR data, in Tables 1 and 2, respectively; HRESIMS *m*/*z* 786.3094 ($[M+H]^+$, calcd for $C_{41}H_{52}N_7O_9$, 786.3827).

4.5. Per-N-methylation of 6

Iodomethane (0.15 mL, 2.4 mmol), tetrabutylammonium iodide (28.1 mg, 0.0761 mmol), and powdered NaOH (60 mg, 1.5 mmol) were added to a solution of **6** (29.9 mg, 0.0380 mmol) in dichloromethane (0.45 mL), and the mixture was stirred vigorously at room temperature for 24 h. Water (5 mL) was added to the mixture, and the whole was extracted with CH_2Cl_2 (3 × 10 mL). The combined CH_2Cl_2 extracts were washed with brine (5 mL), dried over sodium sulfate, and filtered, and the solvent removed in vacuo. The residue was subjected to HPLC (MeOH/H_2O 70:30) to give **7** (19.3 mg, 62%) as an amorphous solid, $[\alpha]_D^{25}$ −68 (*c* 0.19, $CHCl_3$). IR (film) ν_{max} 3356, 2936, 1649, 1514 cm^{-1}; ^1H and ^{13}C NMR data, in Tables 1 and 2, respectively; HRESIMS *m*/*z* 814.4125 ($[M+H]^+$, calcd for $C_{43}H_{56}N_7O_9$, 814.4140); Analytical HPLC (MeCN/H_2O 55:45, flow rate 0.53 mL/min) 18.3 and 25.1 min.

4.6. Des-N-amination of 7

Sodium nitrite (3.0 mg, 0.043 mmol) was added to a cooled (0 °C) and stirred solution of **7** (17.9 mg, 0.0220 mmol) in tetrahydrofuran/0.1 M aqueous hydrochloric acid (10:1, 1 mL) over 30 min. The mixture was further stirred at 0 °C for 30 min and then at room temperature for 3 h. Water (5 mL) was added to the mixture, and the whole was extracted with $CHCl_3$ (3 × 10 mL). The combined $CHCl_3$ extracts were washed with brine (5 mL), dried over sodium sulfate, and filtered, and the solvent removed in vacuo. The residue was subjected to HPLC (MeCN/H_2O 45:55) to give **4** (8.1 mg, 46%) as colorless prisms, mp 208–211 °C (MeOH), $[\alpha]_D^{25}$ −120 (*c* 0.07, $CHCl_3$). IR (film) ν_{max} 3307, 3006, 2934, 1651, 1515 cm^{-1}; ^1H and ^{13}C NMR data, in Tables 1 and 2, respectively; HRESIMS *m*/*z* 799.4014 ($[M+H]^+$, calcd for $C_{43}H_{55}N_6O_9$, 799.4031).

4.7. Crystallography of 3a and 4

Compound **3a**: $C_{88.52}H_{112.52}Br_2Cl_{1.55}N_{12}O_{18}$; M = 1847.29; 0.24 × 0.20 × 0.15 mm, monoclinic; space group *C*2; a = 30.6207(9) Å; b = 12.3675(4) Å; c = 13.3862(4) Å; β = 109.200(2)°; V = 4787.4 (3) $Å^3$; Z = 2; D_X = 1.282 Mg m^{-3}; μ(Mo Kα) = 0.959 mm^{-1}; 37,271 reflections collected; 12,587 unique (R_{int} = 0.0336), $R1$ = 0.0673, $wR2$ = 0.1844 [$I > 2\sigma(I)$], GOF = 1.021; $R1$ = 0.0880, $wR2$ = 0.1995 (all data), absolute structure parameter 0.029(8).

Compound **4**: $C_{43}H_{54}N_6O_9$, $2(CH_4O)$, M = 863.01, 0.48 × 0.27 × 0.06 mm, orthorhombic, space group $P2_12_12_1$, a = 15.685 (2) Å, b = 15.782(2) Å, c = 18.147(3) Å, V = 4492.2(12) $Å^3$, Z = 4, D_X = 1.276 Mg m^{-3}, μ(Mo Kα) = 0.092 mm^{-1}, 52,252 reflections collected, 10,404 unique (R_{int} = 0.0334), $R1$ = 0.0423, $wR2$ = 0.1198 [$I > 2\sigma(I)$], GOF = 1.033; $R1$ = 0.0436, $wR2$ = 0.1212 (all data).

The structures were solved by direct methods using SHELXS-97,[18] and refined by full-matrix least-squares on F^2 using SHELXL-97.[19] Crystallographic data for compounds **3a** and **4** reported in this paper have been deposited with the Cambridge Crystallographic Data Centre under the reference numbers CCDC 677161 and 795575, respectively. These data can be obtained free of charge via http://www.ccdc.cam.ac.uk/data_request/cif, or by e-mailing data_request@ccdc.cam.ac.uk, or by contacting The Cambridge Crystallographic Data Centre, 12, Union Road, Cambridge CB2 1EZ, UK; fax: +44 1223 336033.

References and notes

1. Itokawa, H.; Takeya, K.; Mihara, K.; Mori, N.; Hamanaka, T.; Sonobe, T.; Iitaka, Y. *Chem. Pharm. Bull.* **1983**, *31*, 1424.
2. Itokawa, H.; Takeya, K.; Hitotsuyanagi, Y.; Morita, H. In *The Alkaloids*; Cordell, G. A., Ed.; Academic Press: NY, 1997; Vol. 49, p 301.
3. Jolad, S. D.; Hoffman, J. J.; Torrance, S. J.; Wiedhopf, R. M.; Cole, J. R.; Arora, S. K.; Bates, R. B.; Gargiulo, R. L.; Kriek, G. R. *J. Am. Chem. Soc.* **1977**, *99*, 8040.
4. Zalacaín, M.; Zaera, E.; Vázquez, D.; Jiménez, A. *FEBS Lett.* **1982**, *148*, 95.
5. Sirdeshpande, B. V.; Toogood, P. L. *Bioorg. Chem.* **1995**, *23*, 460.
6. Fujiwara, H.; Saito, S.; Hitotsuyanagi, Y.; Takeya, K.; Ohizumi, Y. *Cancer Lett.* **2004**, *209*, 223.
7. Bates, R. B.; Cole, J. R.; Hoffmann, J. J.; Kriek, G. R.; Linz, G. S.; Torrance, S. J. *J. Am. Chem. Soc.* **1983**, *105*, 1343.
8. Morita, H.; Kondo, K.; Hitotsuyanagi, Y.; Takeya, K.; Itokawa, H.; Tomioka, N.; Itai, A.; Iitaka, Y. *Tetrahedron* **1991**, *47*, 2757.
9. Itokawa, H.; Kondo, K.; Hitotsuyanagi, Y.; Isomura, M.; Takeya, K. *Chem. Pharm. Bull.* **1993**, *41*, 1402.
10. Itokawa, H.; Saitou, K.; Morita, H.; Takeya, K.; Yamada, K. *Chem. Pharm. Bull.* **1992**, *40*, 2984.
11. Boger, D. L.; Zhou, J. *J. Am. Chem. Soc.* **1995**, *117*, 7364.
12. Hitotsuyanagi, Y.; Suzuki, J.; Takeya, K.; Itokawa, H. *Bioorg. Med. Chem. Lett.* **1994**, *4*, 1633.
13. Gund, P.; Veber, D. F. *J. Am. Chem. Soc.* **1979**, *101*, 1885.
14. Itokawa, H.; Morita, H.; Kondo, K.; Hitotsuyanagi, Y.; Takeya, K.; Iitaka, Y. *J. Chem. Soc., Perkin Trans. 2* **1992**, 1635.
15. Hitotsuyanagi, Y.; Sasaki, S.-i.; Matsumoto, Y.; Yamaguchi, K.; Itokawa, H.; Takeya, K. *J. Am. Chem. Soc.* **2003**, *125*, 7284.
16. Itokawa, H.; Takeya, K.; Mori, N.; Sonobe, T.; Mihashi, S.; Hamanaka, T. *Chem. Pharm. Bull.* **1986**, *34*, 3762.
17. Itokawa, H.; Kondo, K.; Hitotsuyanagi, Y.; Nakamura, A.; Morita, H.; Takeya, K. *Chem. Pharm. Bull.* **1993**, *41*, 1266.
18. Sheldrick, G. M. SHELXS-*97: Program for the Solution of Crystal Structures*; University of Göttingen: Göttingen, Germany, 1997.
19. Sheldrick, G. M. SHELXL-*97: Program for the Refinement of Crystal Structures*; University of Göttingen: Göttingen, Germany, 1997.